

The Maximum Circular Velocity Dependence of Halo Clustering

Contents

1	Introduction	1
2	The Simulation	1
3	The Maximum Circular Velocity Dependence of Halo Clustering	2
3.1	The Maximum Circular Velocity	2
3.2	Samples	2
3.3	Halo Bias	3
4	Applications	5
4.1	Mvir-based v.s. Vmax-based	5
4.2	$\Delta\Sigma(r)$	6
4.3	HOD(?)	7
5	Discussion	7

1 Introduction

The halo model has been remarkably successful in describing observations of galaxy clustering at many scales and many redshifts (give some examples here). fundamental assumption clustering only depends on the halo mass; not true because of assembly bias on large scales but also ideas of e.g.. backsplashed halos. recent trend has been to populate galaxies according to their maximum circular velocity. Describe why this might be motivated — depends only on the central part of the potential, set early in the growth of the halo (point to Frank's recent paper here as an example). Also may be more robust to disruption in mergers.

goal here is to discuss the dependence of galaxy clustering on the central velocity dispersion both on small and large scales. We show that some of the features in a detailed halo model come from the effects of back-splash halos.

2 The Simulation

We use cosmological N-body simulations called the Bolshoi simulation and the MultiDark simulation, described in XXX and XXX respectively, to investigate the maximum circular velocity dependence of halo clustering. The Bolshoi simulation uses 2048^3 particles with a volume of $(250h^{-1}\text{Mpc})^3$, while the MultiDark simulation uses the same number of particles as the Bolshoi simulation but with a volume of $(1h^{-1}\text{Gpc})^3$. Both simulations assumes a flat ΛCDM model with density parameters $\Omega_m = 0.27$, $\Omega_\Lambda = 0.73$, $\Omega_b = 0.0469$, and $\sigma_8 = 0.82$, $n = 0.95$, $h = 0.70$. The details of the simulations are described in XXX. We use both simulations to get large dynamic mass range.

For halo identification, we use the ROCKSTAR halo finder (XXX) where the halo masses and maximum circular velocities are computed from bound particles. For the sake of internal structure of halos to be resolved well enough, we make very conservative cut in mass and maximum circular velocity. We use halos whose mass is greater than $10^{12}h^{-1}\text{M}_\odot$ (corresponding to > 100 particles per halo) and whose maximum circular velocity is greater than 200km/s for the MultiDark simulation and halos whose mass is greater than $10^{11}h^{-1}\text{M}_\odot$ (corresponding to > 740 particles per halo) and whose maximum circular velocity is greater than 95km/s for the Bolshoi simulation. Those values correspond to the peak in the number of halos by binning them as a function of mass and maximum circular velocity. The ROCKSTAR halo finder also provides the merger trees for halos classified into three different categories of halos: host halo, subhalos, and ejected halos. Host halos are the halos which never been within the virial radius of more massive halos. Subhalos are the halos which are within the virial radius of more massive halos at $z = 0$. Ejected halos, sometimes called "backsplash"

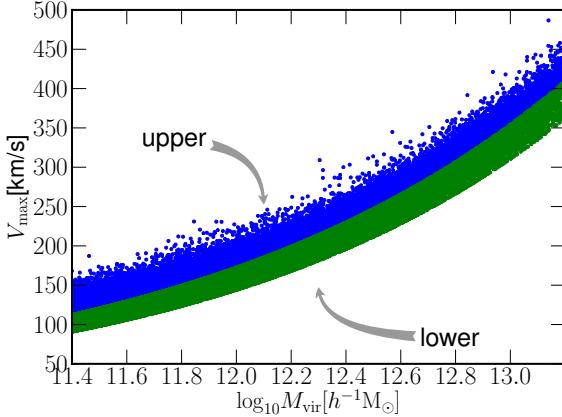


Figure 1. Distribution of halo mass and maximum circular velocity at $z = 0.0$ for halos from the Bolshoi simulation. The blue dots represent halos whose observed maximum circular velocity, $V_{\max,\text{obs}}$, is greater than \bar{V}_{\max} , while the green dots are the ones with smaller $V_{\max,\text{obs}}$ than \bar{V}_{\max} . The boundary between blue and green dots correspond to \bar{V}_{\max} computed from Eq. 3.1.

halos, are the distinct halos at $z = 0$ whose main progenitor passed through the virial radius of a more massive halos at least once in the past.

3 The Maximum Circular Velocity Dependence of Halo Clustering

In this section, we investigate the maximum circular velocity dependence of halo clustering on both large and small scales. We first start with an analytic expression of the maximum circular velocity computed from the halo mass and its concentration. Then, we explain how we select halos to remove the halo mass dependence from the samples using the analytic expression of the maximum circular velocity.

3.1 The Maximum Circular Velocity

Here, we assume that dark matter halos are defined as a spherical halo with a virial radius. Those halos have average density equal to $\Delta_h \rho_{\text{crit}}$ where $\Delta_h = 360$ for the MultiDark and Bolshoi simulations. We also assume that those spherical halos have an NFW density profile (XXX). Then, the maximum circular velocity \bar{V}_{\max} as a function of the halo mass M_{vir} and its concentration c is given by:

$$\bar{V}_{\max} = 0.465 M_{\text{vir}}^{1/3} \sqrt{G(\frac{4}{3}\pi\Delta_h\rho_{\text{crit}}\Omega_m)^{1/3} \frac{c}{\ln(1+c) - c/(1+c)}}. \quad (3.1)$$

The median concentration-mass relation at $z = 0$ obtained from the Bolshoi simulation in Ref. XXX(Klypin et al. 2011) is:

$$\log_{10}c = -0.097\log_{10}M_{\text{vir}} + 2.148. \quad (3.2)$$

By using the above median concentration to Eq. 3.1, we obtain a one to one mapping between the virial halo mass and its maximum circular velocity, denoted as \bar{V}_{\max} hereafter. Given this mapping, we can translate clustering measurements as a function of halo mass into predicted clustering measurements as a function of maximum circular velocity. Our goal below is to determine whether this conversion describes the measured clustering or if there is a residual dependence on the maximum circular velocity.

3.2 Samples

In order to explore a dependence on the maximum circular velocity, we first split the sample into a sequence of virial mass bins, chosen such that there are the same numbers of halos in each bin. This

process is reminiscent of an abundance-matching procedure (cite XXX). We then further split each bin into two subsamples with their observed $V_{\max, \text{obs}}$ greater than (denoted by “upper”) or less than (denoted as “lower”) \bar{V}_{\max} . Fig. 1 shows the distribution of halo mass and maximum circular velocity classified into “upper” (blue dots) and “lower” (green dots) samples as an example. As you can see, the number of halos in each sample is almost half for any halo mass bins. This selection ensures that both the upper and lower subsamples have the same mean halo mass. Therefore, in the absence of an additional M_{vir} dependence on clustering, these samples should have the same clustering properties. Note that this would not be true if we had simply split the sample along V_{\max} , since the two resulting subsamples would have different mean halo masses.

3.3 Halo Bias

We use cross correlation functions to reduce the shot noise effect on the error. In order to measure halo biases, we compute halo-matter cross correlation functions for each subsample and measure a linear bias

$$b_{\text{lin}} = \sum_i (\xi_{hm}(r_i)/\xi_{mm}(r_i))/N_{\text{bin}}, \quad (3.3)$$

where ξ_{hm} and ξ_{mm} are halo-matter and matter-matter correlation functions and we take the average of the ratio on r from $10h^{-1}\text{Mpc}$ to $20h^{-1}\text{Mpc}$, which contains 20 bins as a total. Here, instead of using full DM particles, we subsample 1000000 particles to compute matter auto correlation functions.

In Fig. 2, we show how linear biases depend on the maximum circular velocity as a function of halo mass. We compute linear biases for each mass bin classifying into “upper” and “lower” maximum circular velocity halos. The halos which have different maximum circular velocity have different linear bias values. On large mass end, halos with $V_{\max} < \bar{V}_{\max}$ have a larger linear bias, which is consistent to the result discussed in Ref. XXX(Dalal et al. 2008). On the other hand, as halo masses decrease, halos with $V_{\max} > \bar{V}_{\max}$ start having larger linear biases than those with $V_{\max} < \bar{V}_{\max}$, and the difference between those two samples increases up to 40%. We think that the drop of the ratio on the low mass end is due to mass resolution of the simulation not resolving all the halos for the low mass.

In Fig. 3, we investigate the maximum circular velocity dependence of halo bias on small scales. On small scales, a halo bias is scale-dependent. The question here is whether halos with different maximum circular velocity have different scale-dependence on their biases. In order to find that, we take the ratio of halo-matter cross correlation functions between “upper” and “lower” subsamples and normalize it by their linear biases, shown in Fig. 3. By normalizing by their linear biases, the ratios go to one on large scales. Fig. 3 clearly shows different scale-dependence between “upper” and “lower” subsamples, and the difference becomes larger as halo masses decrease. We particularly see that there is a characteristic bump around 1 to $2 h^{-1}\text{Mpc}$. This implies that many halos in the “upper” samples, especially low mass halos, cluster very closely to each other.

Up to now, we use both host halos and ejected halos to compute halo biases. Both types of halos are identified as distinct halos at $z = 0$. Ejected halos are, however, halos which were identified as a part of a more massive halos at one or more occasions in the past. Those ejected halos tend to exist around a more massive halos (any reference?), and only some of them may be gravitationally bound to other more massive halos. We question how much of the effect in the scale-dependent biases is caused by those ejected halos.

To test this, we compute halo-matter cross correlation functions without the ejected halos. Fig. 4 shows the same figures as Fig. 3 without ejected halos from the Bolshoi simulation. Due to mass resolution, we could not find many ejected halos in the MultiDark simulation. After removing ejected halos, the ratios of linear biases between “upper” and “lower” samples are suppressed by ~10%. There are, however, still more than 25% differences in those samples. Once removing the ejected halos, the deviation of the halo bias on small scales is greatly reduced. On the other hand, the different scale dependence of halo bias appeared on small scales significantly goes down to less than 10%, which implies that difference in small scale halo biases are mostly due to the ejected halos.

We conclude that halos which have different V_{\max} cluster differently even when those halos have the same virial mass. Especially, the scale-dependence of halo biases on small scales shows a significant difference, which mainly caused by the ejected halos.

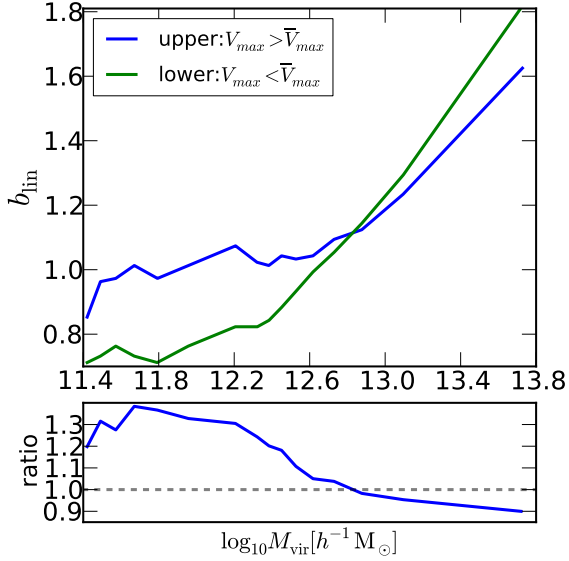


Figure 2. Upper panel: Linear bias at $z = 0.0$ as a function of halo mass from the Bolshoi simulation and the MultiDark simulation. The blue circles corresponds to a linear bias for halos whose maximum circular velocities are greater than \bar{V}_{max} (called “upper” samples in the text), while the green circles correspond to halos whose maximum circular velocities are smaller than \bar{V}_{max} (called “lower” samples). Lower panel: Ratio of linear biases between “upper” (i.e., $V_{\text{max}} > \bar{V}_{\text{max}}$) and “lower” (i.e., $V_{\text{max}} < \bar{V}_{\text{max}}$) samples from the Bolshoi simulation and the MultiDark simulation. As halo masses decrease, the difference on linear bias between “upper” and “lower” samples becomes larger up to 40%.

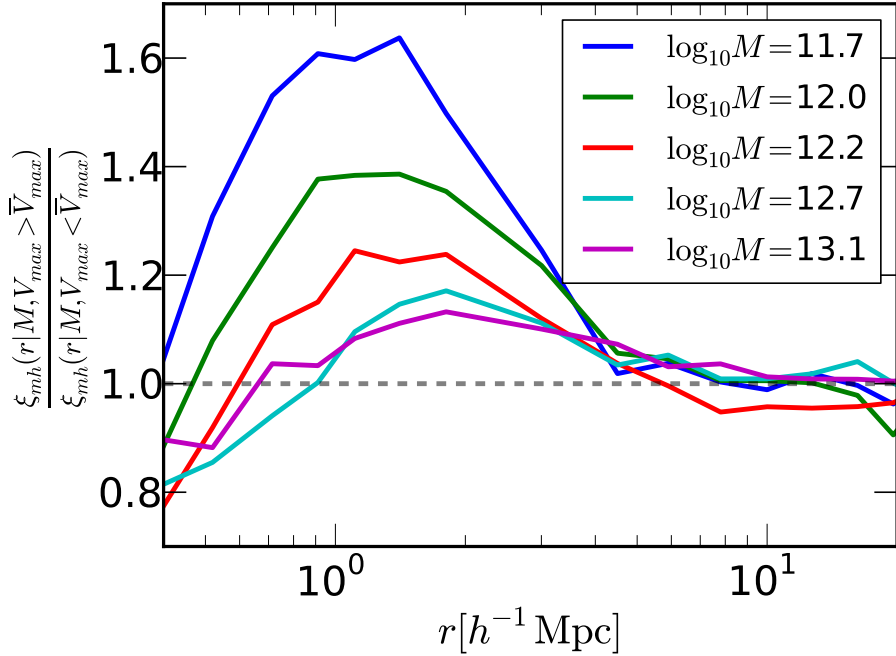


Figure 3. Ratio of halo-matter cross correlation functions between “upper” and “lower” subsamples normalized by their linear biases. The plots are from the Bolshoi simulation and the MultiDark simulation at $z = 0.0$. Each line corresponds to different halo mass bins labeled in the plots. Those plots show that “upper” and “lower” subsamples have different scale-dependence on small scales and the relative scale-dependence between those subsamples increases smoothly with decreasing halo mass.

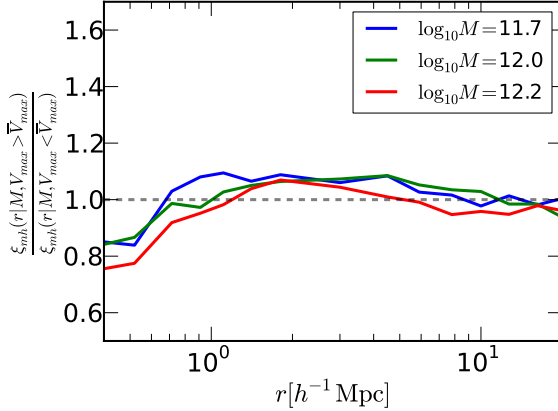


Figure 4. The same figures as Fig. 3 without ejected halos from the Bolshoi simulation. As can be seen by comparing these results to those in Fig. 3, the V_{max} -dependence of halo bias on small scales is dramatically reduced by excluding ejected subhalos. This implies an intimate connection between assembly bias and subhalo back-splashing.

–use jackknife sampling to put error bars

4 Applications

In this section, we demonstrate possible observational relevances of the results in the previous section to complement the halo theory results. We start with the abundance matching (citation?) technique based on halo mass and the maximum circular velocity, and then compute $\Delta\Sigma(R)$ using those two different abundance matching.

4.1 Mvir-based v.s. Vmax-based

In abundance matching, we assume that a big galaxy lives in a big halo in a hierarchical manner to link galaxies to halos. The question is what “big” halos really mean. To rank order halos, we want to identify what kind of physical properties of halos characterize “size” of halos. As a first step, we explore how the abundance matching based on halo mass and maximum circular velocity make difference on halo clustering.

First, we check the correspondence between $\bar{n}(M_{\text{vir}})$ and $\bar{n}(V_{\text{max}})$ as shown in Fig. 5. The red line shows the boundary where $\bar{n}(M_{\text{vir}} <) = \bar{n}(V_{\text{max}} <)$ (how can I phrase this differently?). This boundary overlaps with \bar{V}_{max} from Eq. 3.1, which implies that XXX.

Similar to the previous section, we compute halo-matter cross correlation functions for the abundance matched samples by splitting halos into a sequence of halo mass bins and the maximum circular velocity bins chosen such that each bin has the same number of halos. We observe that the linear biases for the samples $\bar{n}(V_{\text{max}})$ are larger than the ones for the samples $\bar{n}(M_{\text{vir}})$ by 5% with ejected halos, while the difference in linear biases is suppressed to 2% by excluding ejected halos. This result agrees with the result in Sec. 3.2. The magnitude of the difference is, however, smaller than the cases of splitting the samples based on \bar{V}_{max} .

We also compare the cross correlation functions on small scales. Figure 6 is the same as Figure 3 with the ejected halos (left panel) and without the ejected halos (right panel). We see the same trend as the previous section in the different scale dependence between $\bar{n}(M_{\text{vir}})$ and $\bar{n}(V_{\text{max}})$, which is caused mainly by the ejected halos.

- how to describe the result for small scale biases?
- interpretation/implication
- what’s the possible problem if any
- what’s interesting

-check the number of ejected halos in Vmax and Mvir:

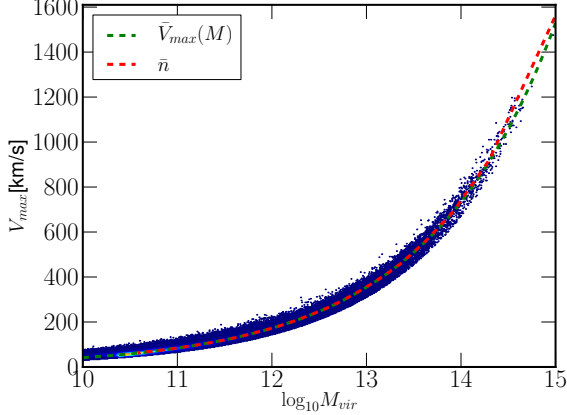


Figure 5. Distribution of halo mass and the maximum circular velocity as a contour plot, overplotted \bar{V}_{\max} (as a green dashed line) and the correspondence between M_{vir} and V_{\max} in abundance matching (as a red dashed line labeled as \bar{n}). The plot shows that \bar{V}_{\max} and the correspondence in abundance matching overlaps on most of halo mass scales.

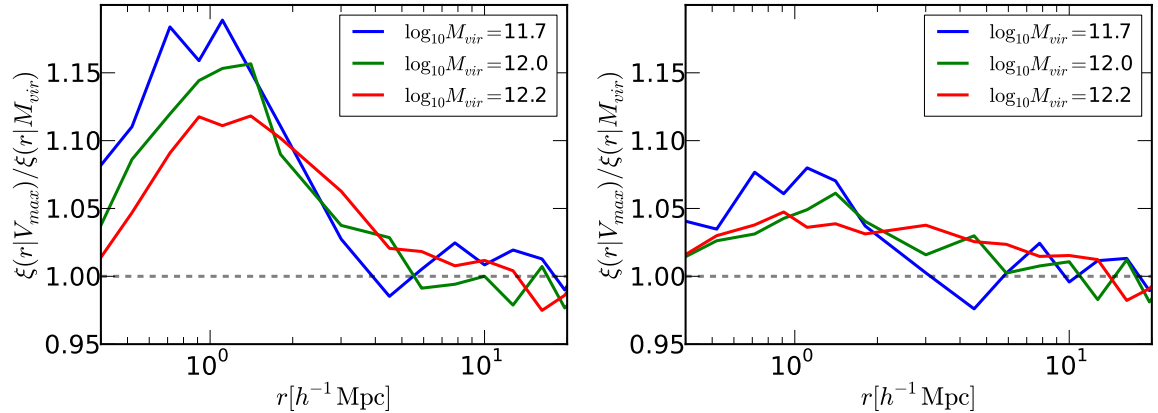


Figure 6. Ratio of halo-matter cross correlation functions between M_{vir} -based and V_{\max} -based abundance matching samples with ejected halos (left) and without ejected halos (right). The ratios are normalized by their linear biases. Each line corresponds to different halo mass bins labeled in the plots (which can be translated into corresponding \bar{V}_{\max} through Eq. 3.1). When samples contain ejected halos, there is a strong scale-dependent difference between those two different abundance matching samples around $1h^{-1}\text{Mpc}$. By excluding ejected halos, the difference is more or less removed.

4.2 $\Delta\Sigma(r)$

(Both are from Andrew's comments)

-Select a bin of Milky Way mass host halos, and select their number-density-matched V_{\max} -selected equivalent. Use Peter Behroozi's stellar-to-halo mass relation to estimate the stellar mass of the central galaxy that would be found in these halos, then plot the halo-matter cross-correlation as a function of scale, over-plotting the two results.

-want to show: We show that the galaxy-galaxy lensing signal of low-mass centrals is impacted at the xxx-yyy% level, in a highly scale-dependent fashion, by the theoretical choice to empirically connect stellar mass to either host halo V_{\max} or M_{vir} .

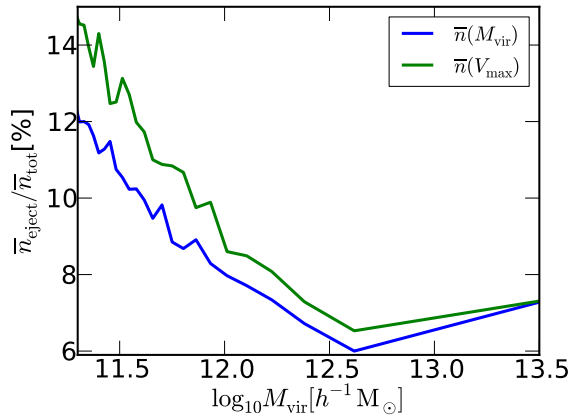


Figure 7. The number of ejected halos as a function of halo mass (need to change either y-label or the plotted object).

4.3 HOD(?)

5 Discussion

(Option)